

# Fission of Heavy Uranium and Thorium isotopes: Source of New Phenomena and Dynamics

L. Satpathy<sup>1,\*</sup>, R.K. Choudhury<sup>2</sup>, and S.K. Patra<sup>1†</sup>

<sup>1</sup>*Institute of Physics, Sachivalaya Marg, Bhubaneswar - 751 005, India and*

<sup>2</sup>*Nuclear Physics Division, Bhabha Atomic Research Centre, Mumbai-400085.*

In view of the energy generation potential of  $^{233}\text{U}$ ,  $^{235}\text{U}$  and  $^{232}\text{Th}$ , we have chosen to study the fission properties of the exotic neutron-rich isotopes  $^{250}\text{U}$ ,  $^{256}\text{U}$ ,  $^{260}\text{U}$ ,  $^{240}\text{Th}$ ,  $^{250}\text{Th}$  and  $^{256}\text{Th}$  in addition to the known  $^{236}\text{U}$  and  $^{232}\text{Th}$  in the valley of stability. Our study has been carried out in the frame work of microscopic relativistic mean field theory and semi-phenomenological analysis of data on fission half-life and fission barrier. It is shown that excess of neutron in these isotopes leads to increase in the fission barrier width giving rise to dramatic enhancement in the stability against spontaneous fission. In the typical case of  $^{250}\text{U}$  the half-life estimated is  $\sim 10^{24}$  years. It shows that these isotopes will undergo a new mode of fission termed *multifragmentation fission* where a number of prompt scission neutron are expected to be simultaneously released along with the two fragments. These are extra neutrons in addition to the usual neutron multiplicity emitted by the two fragments later in the flight. It will have serious implication in the energy generation process in the *r* – *process* nucleosynthesis.

## 1. Introduction

Exploration of new nuclear landscape in the neutron-rich side of the nuclear chart will produce novel nuclear matter with high neutron to proton ratio, a source of new phenomena and dynamics. In view of the energy generation potential of  $^{233}\text{U}$ ,  $^{235}\text{U}$  and  $^{232}\text{Th}$ , we have chosen to study the fission properties of the exotic neutron-rich isotopes  $^{250}\text{U}$ ,  $^{256}\text{U}$ ,  $^{260}\text{U}$ ,  $^{240}\text{Th}$ ,  $^{250}\text{Th}$  and  $^{256}\text{Th}$  in addition to the known  $^{236}\text{U}$  and  $^{232}\text{Th}$  in the valley of stability. Further, the question: how do the fission properties of these exotic neutron-rich isotopes of great relevance in r-process nucleosynthesis change due to the presence of excess neutron compared to the well studied  $^{236}\text{U}$  and  $^{232}\text{Th}$ . Our study has been carried out in the frame work of microscopic relativistic mean field theory and semi-phenomenological analysis of data on fission half-life and fission barrier.

## 2. Thermal fissile property:

$^{233}\text{U}$  and  $^{235}\text{U}$  are the nuclei in the actinide region in the  $\beta$ –stability valley which are ther-

mally fissile and have been mainly used in reactors for power generation. The possibility of occurrence of thermally fissile members in the chain of neutron-rich U and Th isotopes was examined. The neutron number  $N=164$  has been predicted over the last several decades to be magic in numerous theoretical studies. The series of U/Th isotopes around it with  $N = 154 - 172$  were identified to be thermally fissile on the basis of fission barrier and neutron separation energy systematics [1]. We have shown in Fig. 1, these systematics using theoretical predictions of mass formulae and fission barrier calculations.

## 3. Fission barrier profile:

How does the fission barrier profile change due to excess of neutrons in the above isotopes ? The fission decay mode is primarily governed by the profile of the fission barrier which is supposed to be parabolic in nature characterised by both height and width. We adopted a semi-empirical method to get the width of the barrier from the systematics of known experimental fission half-lives and extrapolate them to neutron-rich regions of interest.

The fission half-life can be calculated using the relation [6].

\*Electronic address: [satpathy@iopb.res.in](mailto:satpathy@iopb.res.in)

†Electronic address: [patra@iopb.res.in](mailto:patra@iopb.res.in)

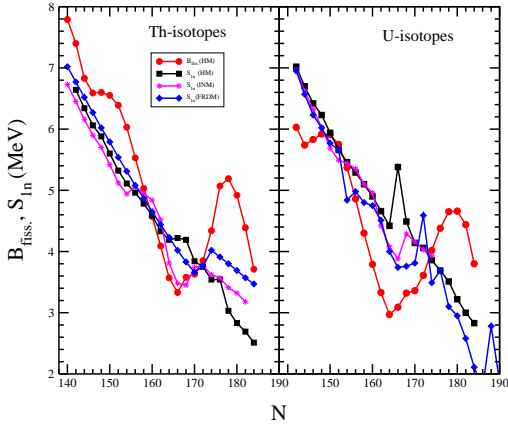


FIG. 1: Fission barrier  $B_f$ , and binding energy of the last neutron  $S_{1n}$  as a function of mass number A for Th and U isotopes. The  $B_f$  are taken from Howard and Möller [2] and  $S_{1n}$  are taken from Refs. [2], [3] and [4] for HM, INM and FRDM model respectively. The neutron separation energy predicted by all the three models predict a general pattern. In all the three cases the fission barrier lies below the neutron single particle energy in the region  $N = 154 - 172$ , which will be vulnerable to thermal neutron fission [5].

$$\tau_{1/2} = \ln 2 / np, \quad (1)$$

where  $n$  is the number of barrier assault by the decaying nucleus, which is related to the barrier curvature energy  $\hbar\omega$  by

$$n\hbar = \hbar\omega / 2\pi, \quad (2)$$

and  $p$  is the penetrability of the barrier given by

$$p = [1 + \exp(2\pi B_f / \hbar\omega)]^{-1}. \quad (3)$$

It may be noted that  $\hbar\omega$  is a measure of the width of the barrier; smaller the value of  $\hbar\omega$  larger is the barrier width. Taking the theoretical values [2] of  $B_f$  and using the experimental  $\tau_{1/2}$  [7], we get the values of  $\hbar\omega$ , which are plotted in Fig. 2 for six actinide elements. It is quite revealing that the plot shows linear behavior of  $\hbar\omega$  with  $B_f$  for a given element. For a typical case of  $^{250}\text{U}$  with  $B_f = 4.3$  MeV we

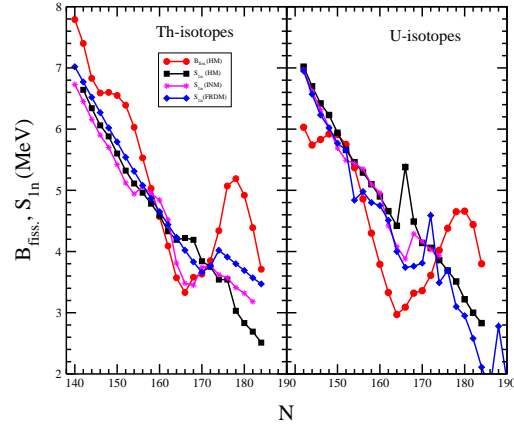


FIG. 2: The barrier width  $\hbar\omega$  as function of fission barrier  $B_f$ . The  $B_f$  values and the experimental half-lives taken from Howard and Möller [2] and Ref. [4], respectively have been used to extract the barrier widths of all the known nuclei showing fission decay in the actinide region. This Figure shows that for each element  $\hbar\omega$  and  $B_f$  show a linear relationship through a straight line behavior depicted in the figure. The star on the line for Uranium in figure, denotes the value of  $\hbar\omega$  to be 0.225 MeV for its  $B_f = 4.3$  MeV corresponding to  $^{250}\text{U}$  [5].

obtained  $\hbar\omega = 0.225$  MeV considerably lower than that of  $^{236}\text{U}$  with  $\hbar\omega = 0.3257$  MeV. The normal nuclei like  $^{230,232}\text{Th}$  and  $^{235,238}\text{U}$  have  $\hbar\omega \approx 0.4 - 0.5$  MeV. Thus excess of neutrons give rise to flattening of the fission barrier making the nucleus stable against spontaneous fission because of decreasing penetrability. For  $^{250}\text{U}$ , we obtained  $\tau_{1/2} = 5.7 \times 10^{24}$  years. However, due to decrease of fission barrier to 4.3 MeV with minute inducement by a thermal neutron, fission decay will occur. This exotic feature results from the excess of neutrons not seen in normal nuclei in the valley of stability.

#### 4. Mechanism of fission from anatomy study of neck:

From the early days the two goals of nuclear theory were to explain the fission phenomena and the working of the nuclear independent particle model in terms of Hamiltonian involv-

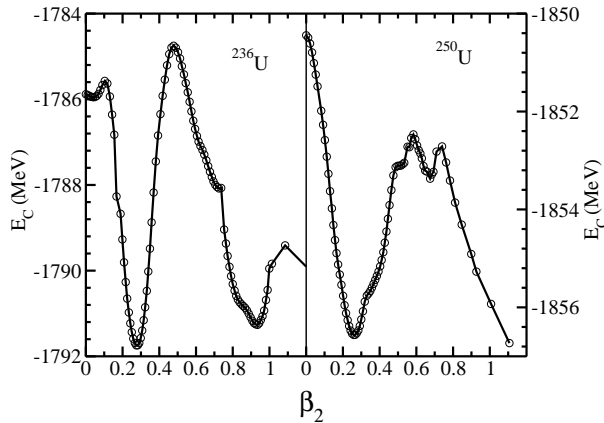


FIG. 3: The energy curves of  $^{236}\text{U}$  and  $^{250}\text{U}$  as a function of the deformation parameter  $\beta_2$  obtained in the Relativistic mean field formalism with NL3 parameter set [5].

ing nucleon-nucleon interaction. Although, the latter goal is more or less reached, the former is still languishing in the mid-way. The effort here is to address this question. We have entertained the specific objective of studying the neck configuration following the static fission path [8] with the hope of unravelling new phenomena and dynamics.

#### A. Static fission path leading to dumbbell neck configuration

Using NL3 interaction in the RMF theory calculation is done for the static fission path in the well studied  $^{236}\text{U}$  and  $^{232}\text{Th}$  allowing only quadrupole deformation for the nucleus to acquire on its way to scission. In Fig. 3, we have plotted the energy as a function of deformation parameter  $\beta_2$  for these two nuclei. It can be seen that the fission barrier for  $^{236}\text{U}$  comes out to be 6.95 MeV comparable to the experimental value of 5.75 MeV. The fission barrier of 4.05 MeV in the case of  $^{250}\text{U}$  obtained in our calculation agrees with the Howard-Möller [2] value of 4.3 MeV. The double-humped fission barrier in both cases have been reproduced. We have presented in Fig. 4 the matter density distributions of some typical configurations of these two nuclei acquire right upto neck configuration. It can be

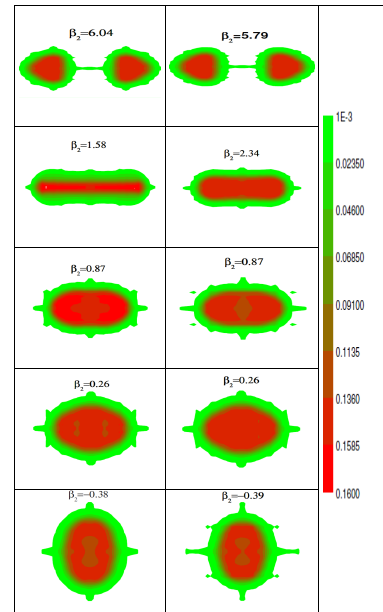


FIG. 4: Evolution of neck for the isotopes of Uranium and Thorium. The matter density distributions for different deformation  $\beta_2$  of  $^{236}\text{U}$  and  $^{232}\text{Th}$  obtained in the relativistic mean field formalism using NL3 parameter set. The total (neutron+proton) number density  $\rho = \rho_n + \rho_p$  in  $\text{fm}^{-3}$  is shown [5].

seen that microscopic calculations of static fission path leading to dumbbell configurations before the scission justify for the first time the classical liquid-drop picture of fission.

#### B. Characteristic of neck

In Table 1, we have presented the energy, deformation, rms radius of the ground state and neck configuration of the two known nuclei  $^{236}\text{U}$  and  $^{232}\text{Th}$  in the valley of stability and the six neutron-rich nuclei  $^{250}\text{U}$ ,  $^{256}\text{U}$ ,  $^{240}\text{Th}$ ,  $^{250}\text{Th}$  and  $^{256}\text{Th}$  away from it. The experimental values wherever known are given in parenthesis. The neck configurations lie around 20 MeV below the corresponding ground state. The ground state rms charge radii for all nuclei are 6 fm and those of the neck configurations around 12 fm. These results are in conformity with our notion of fission dynamics. In Figs. 5 and 6, the matter

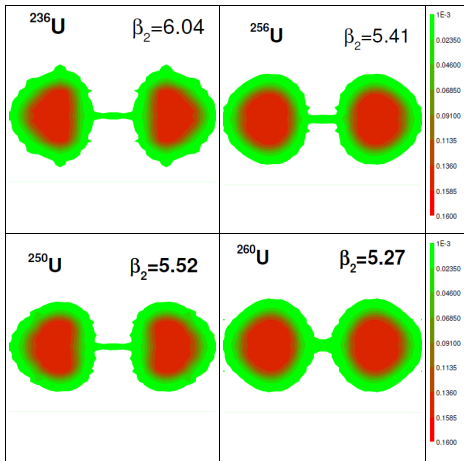


FIG. 5: Evolution of neck for the isotopes of Uranium and Thorium. The matter density distributions for different deformation  $\beta_2$  of  $^{236}\text{U}$  and  $^{232}\text{Th}$  obtained in the relativistic mean field formalism using NL3 parameter set. The total (neutron+proton) number density  $\rho = \rho_n + \rho_p$  in  $\text{fm}^{-3}$  is shown [5].

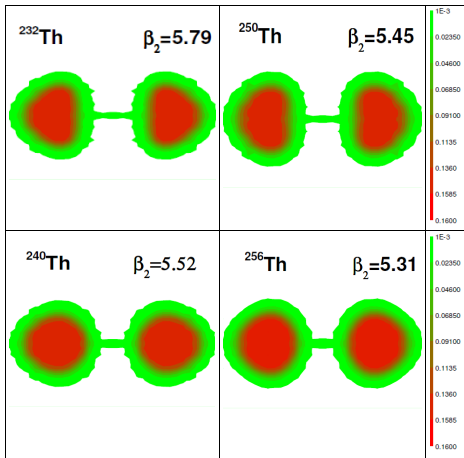


FIG. 6: Same as Figure 5, but for Thorium isotopes [5].

density distributions of the neck configuration obtained in our calculations for U and Th isotopes are presented.

The total number of neutrons  $N_{neck}$  and number of protons  $Z_{neck}$  contained in the neck are obtained by integrating the corresponding

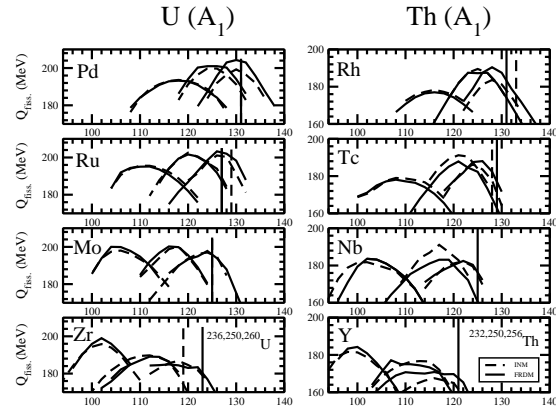


FIG. 7:  $Q_{fiss.}$ -value distribution given by  $Q_{fiss.} = BE(A_1, Z_1) + BE(A_2, Z_2) - BE(A, Z)$  for  $^{236,250,260}\text{U}$  and  $^{232,250,256}\text{Th}$  as a function of  $A_1$  fragment in the binary decay  $A \rightarrow A_1 + A_2$ . The binding energy used for calculation of  $Q$ -value is taken from [4] and Refs. [3] for FRDM and INM, respectively. The fission yield decreases drastically with increase or decrease of mass number of given element. Therefore, we have shown the distribution in the range 90 to 100% of the peak value in each case. The vertical line marks the neutron drip-line for the corresponding element in each panel. The full and dashed line denote the calculations with FRDM and INM mass models respectively [5].

calculated densities over the physical dimension of the neck. In Table 2, these quantities along with the charge radii of the neck, the length  $l_n$ , the tip to tip distance are presented. Thus, our study of the anatomy of neck configurations in terms of the neutron-proton composition shows the progressive rise in the neutron component with increase of mass number. The neutron to proton ratio in U-isotopes increases in the neck from 2.54 ( $^{236}\text{U}$ ) to 4.96 ( $^{260}\text{U}$ ) and in Th from 2.59 ( $^{232}\text{Th}$ ) to 5.55 ( $^{256}\text{Th}$ ). In nuclear matter inhabiting neck region in the heaviest isotope  $^{260}\text{U}$  considered here has the neutron to proton ratio 5:1 which correspond to  $^6\text{H}$  system, the last known quasi-stable (resonance) isotope of half-life 290 yoctosecond of Hydrogen. Since the still heavier isotope of hydrogen are unlikely to be found in nature, it is reason-

TABLE I: The RMF(NL3) results for binding energy BE, the quadrupole deformation parameter  $\beta_2$  and *rms* radius for both the ground and neck configurations for  $^{236}\text{U}$ ,  $^{250}\text{U}$ ,  $^{256}\text{U}$ ,  $^{260}\text{U}$ ,  $^{232}\text{Th}$ ,  $^{240}\text{Th}$ ,  $^{250}\text{Th}$  and  $^{256}\text{Th}$ . The experimental values wherever known are given in parenthesis [5].

Nucleus	State	$\beta_2$	$r_c(fm)$	BE (MeV)
$^{236}\text{U}$	Ground	0.26 (0.28[9])	5.86 (5.84 [10])	1790.5 (1790.4 [11])
	Neck	6.04	12.14	1808.5
$^{250}\text{U}$	Ground	0.26	5.82	1856.5
	Neck	5.52	11.91	1890.7
$^{256}\text{U}$	Ground	0.18	5.97	1880.6
	Neck	5.41	11.78	1914.7
$^{260}\text{U}$	Ground	0.15	5.99	1895.3
	Neck	5.37	11.74	1923.9
$^{232}\text{Th}$	Ground	0.26 (0.26[9])	5.83 (5.71 [10])	1767.1 (1766.7[11])
	Neck	5.79	11.88	1789.0
$^{240}\text{Th}$	Ground	0.26	5.90	1806.3
	Neck	5.52	11.66	1825.2
$^{250}\text{Th}$	Ground	0.22	5.93	1846.3
	Neck	5.45	11.84	1872.2
$^{256}\text{Th}$	Ground	0.16	5.96	1868.8
	Neck	5.31	11.72	1891.5

TABLE II: The Characteristics of neck configuration. The average neutron and proton densities  $\bar{\rho}_n(fm^{-3})$ , and  $\bar{\rho}_p(fm^{-3})$  and their ratios  $\bar{\rho}_n/\bar{\rho}_p$ , number of neutron and proton  $N_{neck}$  and  $Z_{neck}$  contained in the neck, rms charge radius  $r_c^{nk}(fm)$ , length of the neck  $L_n(fm)$ , the centre to centre distance  $l_{cc}(fm)$  and tip to tip distance of the neck  $L_t(fm)$  are presented [5].

Nucleus	$\bar{\rho}_n$	$\bar{\rho}_p$	$\bar{\rho}_n/\bar{\rho}_p$	$Z_{neck}$	$N_{neck}$	$\frac{N_{neck}}{Z_{neck}}$	$r_c^{nk}$	$L_n$	$l_{cc}$	$L_t$
$^{236}\text{U}$	0.058	0.034	1.70	0.95	2.42	2.54	12.14	6.28	21.88	37.48
$^{250}\text{U}$	0.074	0.031	2.37	0.86	3.23	3.75	11.91	5.82	21.56	37.30
$^{256}\text{U}$	0.085	0.031	2.74	0.82	3.77	4.59	11.78	5.46	21.30	37.14
$^{260}\text{U}$	0.093	0.031	3.00	1.03	5.11	4.96	11.74	4.29	21.18	37.07
$^{232}\text{Th}$	0.062	0.041	1.51	0.66	1.71	2.59	11.88	5.18	21.80	38.42
$^{240}\text{Th}$	0.071	0.042	1.69	0.69	2.47	3.57	11.86	4.76	21.44	38.12
$^{250}\text{Th}$	0.081	0.034	2.38	0.62	2.94	4.74	11.82	4.68	21.10	37.52
$^{256}\text{Th}$	0.090	0.033	2.73	0.68	3.78	5.55	11.72	4.52	20.74	36.96

able to conclude such nuclear liquid is not viable. Therefore, neck formation in somewhat heavier than  $^{260}\text{U}$  requiring such nuclear liquid with higher neutron to proton ratio 5:1 will be unsustainable, which signals the breakdown of usual liquid-drop picture of fission visualise so far. So, neck can not be formed and fission will be inhibited in such heavy neutron-rich isotopes. This effect is also manifested in progressive shrinking of the length of the neck with rise of neutron number (See Table 2 and Figs. 5 and 6) which may eventually disappear with increase of mass. The predominant

mode of decay of such nuclei will be  $\beta$ -decay which is a parallel process to the case of superheavy elements in the valley of stability where  $\alpha$ -decay becomes more preferred mode than fission. Thus the general notion that  $r$ -process is eventually terminated by fission seems untenable.

### 5. Multifragmentation fission: a new mode of fission decay

Since neck is the most sensitive part where rupture takes place giving rise to two heavy fission fragments, its composition will play a

crucial role in determining the fission dynamics. In widely studied  $^{236}\text{U}$ , the decay process is binary; at the instant of the rupture of the neck, each of two protruding parts originating from the rupture of the neck is sucked in by the respective connecting fragments. Then the two fragments move in opposite direction, being repelled by the mutual Coulomb repulsion, and emit 2.5 neutrons in the process of de-excitation to the respective ground-states. The sucking of the half of the neck by a fragment is possible because of the presence of sizable number of protons (as shown in the present calculations) in the neck providing attractive nuclear force. However in the heavier isotopes like  $^{250}\text{Th}$ ,  $^{256}\text{Th}$ ,  $^{250}\text{U}$ ,  $^{256}\text{U}$  and  $^{260}\text{U}$  the proton components are relatively smaller compared to the neutron components. The likely scenario in such a system is that the triplet-triplet and singlet-singlet components of the triplet-triplet and singlet-singlet components of nucleon-nucleon force which are repulsive in nature become dominant, and therefore sucking in is unlikely to happen, and the ruptured neck may not be able to hold on all the neutrons, and may simultaneously release them along with the production of the two fragments. This will be a new mode of fission decay as mentioned in the introduction known as *multifragmentation fission* proposed earlier by the authors [5]. In such cases, the multiplicity of neutron will consist of two parts: the usual prompt neutrons plus the multifragmentation neutrons generated at the time of scission contributed by the neck. Taking into account the neck neutrons calculated above, and assuming the modest value of 2.5 for prompt neutrons similar to that of  $^{236}\text{U}$ , the multiplicities are expected to be more than 4 for  $^{250}\text{U}$ ,  $^{256}\text{U}$ ,  $^{260}\text{U}$ ,  $^{250}\text{Th}$  and  $^{256}\text{Th}$ . This prediction will get strong support from the probability of fragment mass-yield as shown below.

The important driving force for the decay of a nucleus is the Q-value of the reaction. The probability of fragment mass-yield in fission process is directly related to the Q-value and temperature at the scission point. We therefore calculate the Q-value systematics of the fission of the nucleus  $(A, Z)$  de-

caying to  $(A_1, Z_1)$  and  $(A_2, Z_2)$  defined as:  $Q_{fiss.}(A, Z) = BE(A_1, Z_1) + BE(A_2, Z_2) - BE(A, Z)$ . To avoid clumsiness we have plotted the Q-values in Fig. 7 for the 6 isotopes  $^{236,250,260}\text{U}$  and  $^{232,250,256}\text{Th}$  for the possible binary decays  $(A, Z) = (A_1, Z_1) + (A_2, Z_2)$  taking even values of  $Z_1$  in the range 39 to 46, with varying  $A_1$ , the complementary fragment  $(A_2, Z_2)$  being thereby fixed. Since the yield falls rapidly with the decrease of the Q-value for an element, the values lying above 90% of the height value are only relevant.

For the present study we have used the masses predicted in the finite range droplet model (FRDM) [4] and infinite nuclear mass model (INM) [3, 12, 13]. We have chosen the latter mass model for its unique success in describing the saturation properties [14] of INM, shell quenching [15] in the large neutron  $N=82, 126$  shells and its long range predictive ability especially in the neutron rich side [16]. It is interesting to see that except three isotopes  $^{232}\text{U}$ ,  $^{236}\text{U}$  and  $^{240}\text{Th}$  in the valley of stability in the remaining five cases the drip-lines fall within the Q-value distributions with a few touching the outer fringe. All the isotopes lying to the right to the drip-line will be unstable against instantaneous release of neutrons from fragments at scission. In the usual fission of  $^{236}\text{U}$ , neutrons will be emitted from the fragments after they are fully accelerated. But, in the heavier neutron-rich isotopes a certain number of neutrons will be simultaneously produced along with the two heavy fragments signalling a new mode of fission decay which we call multifragmentation fission. These are extra neutrons in addition to the usual neutrons multiplicity emitted by the two fragments latter in flight. It will have serious implications in the energy generation process in  $r$ -process nuclear synthesis in stellar evolution. Whether this process will be of any utility in the laboratory is too premature to speculate at the moment.

## 6. Conclusions

Our comparative fission study of  $^{236}\text{U}$  and  $^{232}\text{Th}$  with the six neutron-rich isotopes reveals the following new phenomena

(i) Excess neutron broadens the fission barrier.

(ii) Stability against spontaneous fission is enhanced dramatically. Fission half-life of  $^{250}\text{U}$  is estimated to be  $5.7 \times 10^{24}$  years.

(iii) The neutron to proton ratio in the neck increases with the increase of neutron number in the isotope. In  $^{260}\text{U}$  the ratio is found to be 5:1.

(iv) The liquid-drop picture breaks down due to high neutron to proton ratio in the neck as such nuclear liquid is unstable. Thus fission is inhibited in heavier than  $^{260}\text{U}$  isotopes and the predominant mode of decay of such nuclei will be  $\beta$ -decay rather than fission. So the general notion that  $r$ -process is eventually terminated by fission is untenable.

(v) A new mode of fission decay termed *multifragmentation fission* is predicted for neutron-rich U and Th isotopes.

## References

- [1] L. Satpathy, S.K. Patra and R.K. Choudhury, PRAMANA **70** (2008) 87; K.S. Jayaraman, Nature India **20** May 2008.
- [2] W.M. Howard and P. Möller, At. Data and Nucl. Data Tables, **25** (1980) 219.
- [3] R.C. Nayak and L. Satpathy, At. Data and Nucl. Data Tables, **73** (1999) 213.
- [4] P. Möller, R.J. Nix, W.D. Myers and W.J. Swiatecki, At. Data and Nucl. Data Tables, **59** (1995) 185; P. Möller, R.J. Nix and K.-L. Kratz, At. Data and Nucl. Data Tables, **66** (1997) 131.
- [5] S.K. Patra, R.K. Choudhury and L. Satpathy, J. Phys. G: Nucl. Part. Phys. **37** (2010) 1.
- [6] R. Vandenbosch and J.R. Huizenga, Nuclear Fission, Academic press, inc. (1973) Ch. III, p. 45.
- [7] N.E. Holden and D.C. Hoffman, Pure Appl. Chem. **72** (2000) 1525.
- [8] S.K. Patra, F.H. Bhat, R.N. Panda, P. Arumugam, R.K. Gupta, Phys. Rev. **C79** (2009) 044303.
- [9] S. Raman, C.W. Nestor and P. Tikkanen, At. Data and Nucl. Data Tables **78** (2001) 1.
- [10] I. Angeli, At. Data and Nucl. Data Tables **87** (2004) 185.
- [11] G. Audi, A.H. Wapstra and C. Thibault, Nucl. Phys. **A729** (2003) 337.
- [12] L. Satpathy, J. Phys. **G13** (1987) 761.
- [13] R.C. Nayak, V.S. Uma Maheswari and L. Satpathy, Phys. Rev. **C52** (1995) 711.
- [14] L. Satpathy, V.S. Uma Maheswari and R.C. Nayak, Phys. Rep. **319** (1999) 85.
- [15] L. Satpathy and R.C. Nayak, J. Phys. **G24** (1998) 1527.
- [16] L. Satpathy and S.K. Patra, J. Phys. **G30** 771 (2004) 771.